

COMPARING VOLCANIC TERRAINS ON VENUS AND EARTH: HOW PREVALENT ARE PYROCLASTIC DEPOSITS ON VENUS? L. M. Carter¹, B. A. Campbell², and L. S. Glaze¹, ¹NASA Goddard Space Flight Center (Planetary Geodynamics Lab, NASA Goddard Space Flight Center, Greenbelt, MD 20906; lynn.m.carter@nasa.gov), ²Smithsonian Institution (Center for Earth and Planetary Studies, MRC 315, PO Box 37012, Washington DC 20013)

Introduction: In the last several years, astronomers have discovered several exoplanets with masses less than 10 times that of the Earth [1]. Despite the likely abundance of Earth-sized planets, little is known about the pathways through which these planets evolve to become habitable or uninhabitable. Venus and Earth have similar planetary radii and solar orbital distance, and therefore offer a chance to study in detail the divergent evolution of two objects that now have radically different climates. Understanding the extent, duration, and types of volcanism present on Venus is an important step towards understanding how volatiles released from the interior of Venus have influenced the development of the atmosphere. Placing constraints on the extent of explosive volcanism on Venus can provide boundary conditions for timing, volumes, and altitudes for atmospheric injection of volatiles. In addition, atmospheric properties such as near-surface temperature and density affect how interior heat and volatiles are released.

Radar image data for Venus can be used to determine the physical properties of volcanic deposits, and in particular, they can be used to search for evidence of pyroclastic deposits that may result from explosive outgassing of volatiles. For explosive volcanism to occur with the current high atmospheric pressure, magma volatile contents must be higher than is typical on Earth (at least 2-4% by weight) [2,3]. In addition, pyroclastic flows should be more prevalent on Venus than convective plumes and material may not travel as far from the vent source as it would on Earth [3]. Areas of high radar backscatter with wispy margins that occur near concentric fractures on Sapho Patera [4] and several coronae in Eastern Eistla Regio [5] have been attributed to collapse of eruption columns and runout

of rough materials [6].

Fine-grained pyroclastic deposits are typically dark in radar images due to their smooth surface and lack of embedded rocks. They also often have very low circular polarization ratio (CPR) values. The CPR is the ratio of power in the same sense of circular polarization as was transmitted to the opposite sense circular polarization. Smooth surfaces like ash deposits, smooth pahoehoe flows, or ponded lava have CPR values of <0.2, while rugged blocky lava flows have CPR values from 0.6 to over 1.0 (for incidence angles between 20-40°) [7,8]. Many volcanic flows on Venus have CPR values <0.3, similar to terrestrial pahoehoe flows or smoother a'a flows [7]. Because radar-dark, low CPR terrains can be generated by both pyroclastics and smooth flows, we introduce additional polarimetry measurements to search for pyroclastic deposits.

Data Sets: The Magellan mission to Venus provided single polarization radar imaging of 98% of the planet at a resolution of 150 m/pixel. We have also used the Arecibo Observatory radar to obtain dual-polarization radar data of Venus at a resolution of ~1-3 km. Unlike Magellan, the Arecibo data can be used to generate polarimetry products with a resolution of ~3-12 km [9].

In addition to the CPR (Fig1, below), we also produce maps of the degree of linear polarization (DLP). The DLP is can be used to infer the presence of subsurface scattering. A circularly polarized incident wave can be thought of as a combination of two orthogonal linear vectors that are vertically (V) and horizontally (H) polarized with respect to the plane of incidence. If this wave penetrates the surface, the V polarization will be preferentially transmitted, and the polarization state incurs an additional linear component. Used to-

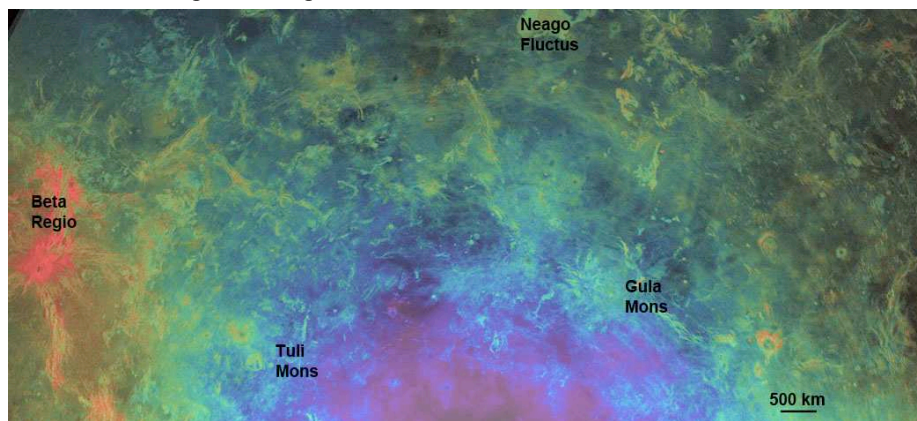


Figure 1: Radar circular polarization maps of Venus derived from ground-based imaging reveal varying textures in volcanic areas such as Gula and Tuli Montes [7,10]. In this image, the CPR has been stretched to a color scale between 0 (purple) and 1 (red) and overlaid on the total radar power. The CPR value increases with higher radar incidence angle; the sub-radar point with nadir incidence is at the lower center of the image.

gether, these polarization products can reveal which components of the radar echo are from the surface or subsurface, and can distinguish between surfaces that are smooth or rough at the wavelength scale [10].

Tuli Mons: An example of possible pyroclastics

Shield volcanism is prevalent on the Venus plains, and prior work has indicated high degree of linear polarization areas associated with many shield fields [9]. One of these sites is Tuli Mons, located at 17.5° N and 313° E (incidence angle $\sim 20^{\circ}$). Magellan SAR images of this area (Fig 2a) reveal dozens of small shields and lava flows with a range of backscatter values.

When the polarization parameters are presented together (Fig. 2b), a more informative picture emerges of this region. The brightest flows have average CPR values of 0.2 but DLP values near 0, suggesting that they are rougher and unmantled. The center part of Tuli Mons has an average CPR value of 0.09, similar to values for lunar pyroclastic deposits at similar incidence angles [11] and to smooth pahoehoe flows [7]. These low CPR areas also have enhanced DLP values (0.08) consistent with penetration of the radar wave into a fine-grained mantling deposit. The highest DLP values (0.13) are associated with flow complexes north of Uilata Fluctus that also have some of the locally highest CPR values (0.2). In this case it is possible that rough flows have been partially mantled by fine material, or the resolution may be too low to distinguish the properties of the smaller flow units. Some radar-bright flows, including Koti Fluctus, have both low CPR and low DLP values, indicating unmantled surfaces that may have formed from ponding or very smooth pahoehoe type flows.

Fine-grained mantling material capable of generating enhanced DLP values can be deposited through volcanic or aeolian processes, or can be formed in place due to physical or chemical breakdown of the surface. However, given the correlation of the low CPR, enhanced DLP areas with the central dome fields of Tuli Mons and Uilata Fluctus, the existence of fine-grained pyroclastics seems plausible. As this work progresses, mapping of low CPR and enhanced DLP areas will provide quantitative information about the spatial distribution of possible pyroclastic deposits.

Future work: Polarimetric radar data of Venus demonstrate that there are a wide variety of volcanic surfaces on Venus, including possible pyroclastic deposits. However, modern orbital radar systems deployed for solid earth studies are producing high-resolution data sets that contain much more information, including full polarimetry, interferometry, and/or multiple wavelengths. These additional techniques, applied to the other terrestrial planets, would provide a dramatic view of recent surface changes, volcanic de-

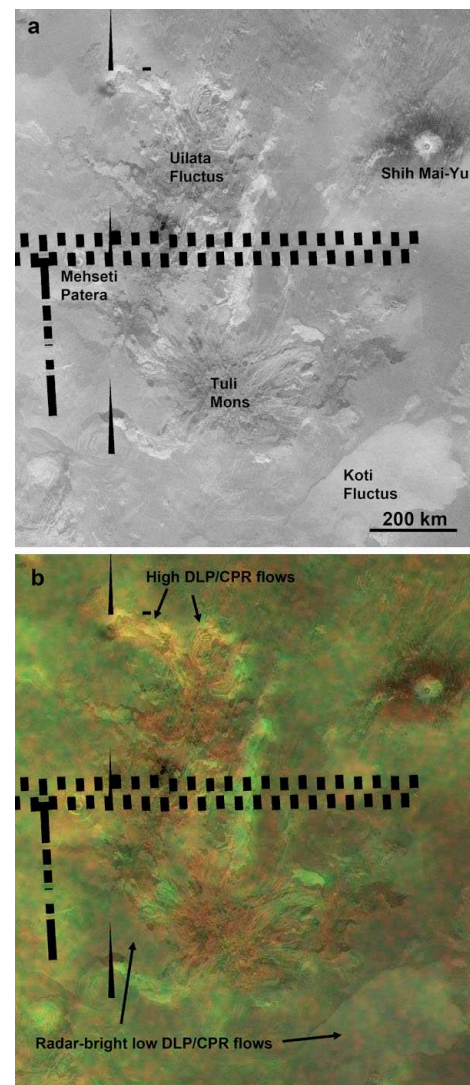


Figure 2: a.) A Magellan SAR image of Tuli Mons. b.) Radar polarimetry overlaid on the Magellan image. Red is the degree of linear polarization and green is the circular polarization ratio. Red areas have low CPR and enhanced DLP that indicate the likely presence of smooth mantling deposits.

posit type, morphology and stratigraphy, and the topography of volcanic centers.

Acknowledgement: This work was supported through a NASA Planetary Geology and Geophysics grant to L. Carter.

References: [1] <http://exoplanets.eu> (4/2012) [2] Garvin, J. B. et al. (1987) *Icarus*, 52, 365. [3] Glaze, L. S. et al. (2011) *JGR*, 116, E01011, doi:10.1029/2010JE003577. [4] McGill, G. E. (2000), USGS Sci. Inv. Map 2637, 2000. [5] Campbell, B.A., and D.A. Clark (2006), USGS Sci. Inv. Map 2897. [6] Campbell, B.A., et al. (1998), LPSC XXIX, Abs. 1810. [7] Campbell, B. A. and D. B. Campbell (1992) *JGR*, 97, 16293. [8] Campbell, B. A. et al. (1993) *JGR*, 98, 17099. [9] Carter, L. M. et al. (2006) *JGR*, 111, E06005, doi:10.1029/2005JE002519. [10] Carter et al. (2011) *Proc IEEE*, 99, doi:10.1109/JPROC.2010.2099090. [11] Carter et al. (2009) *JGR*, 114, E11004, doi:10.1029/2009JE003406.